Direct Observation of Dislocation Core Structures in CdTe/GaAs(001)

A. J. McGibbon,* S. J. Pennycook, J. E. Angelo†

A strategy is presented for determining sublattice polarity at defects in compound semiconductors. Core structures of 60-degree and Lomer dislocations in the CdTe/GaAs(001) system have been obtained by the application of maximum-entropy analysis to *Z*-contrast images (*Z* is atomic number) obtained in a 300-kilovolt scanning transmission electron microscope. Sixty-degree dislocations were observed to be of the glide type, whereas in the case of Lomer dislocations, both a symmetric (Hornstra-like) core and an unexpected asymmetric structure made up of a fourfold ring were seen.

Of critical importance in the understanding of the transport and optoelectronic properties of semiconductor devices is a knowledge of the precise atomic arrangements at dislocations in fabricated materials. Although many models for dislocation core structures in diamond-cubic–based lattices have been proposed [see, for example, (*1*–*4*)], direct observation has not been possible. Interpretation of experimental evidence has therefore relied on the properties of preconceived, nonunique atomic models as corroboration (*5*). Using Z-contrast imaging on a 300-kV scanning transmission electron microscope (STEM) in conjunction with maximum-entropy image analysis, we have acquired directly interpretable atomic resolution images of dislocation core structures in compound semiconductors. Besides the crucial ability to directly distinguish glide and shuffle dislocations, we demonstrate the existence of unexpected core structures. Insight into the dislocation core structures of polar semiconductors represents an important step toward an understanding of their electronic and optical properties.

One system in which dislocations play a crucial role (*6*) is that of $Cd_xHg_{1-x}Te$ (CMT), which is used in a broad range of infrared optoelectronic applications, including, for example, two-dimensional focal-plane detector arrays (*7*). In the fabrication of CMT systems, there has been considerable interest in the use of relatively inexpensive GaAs(001) substrates [see, for example, (*8*, *9*)]. However, because of the large lattice mismatch that exists between GaAs and CdTe, a wide variety of defect structures can occur that can, in turn, seriously affect device performance.

In the investigation of the interrelation among growth conditions, materials structure, and electronic properties in highly mismatched III-V/II-VI heteroepitaxial systems, the growth of CdTe on GaAs(001) provides an ideal model system (*10*–*12*). The CdTe can be grown epitaxially on GaAs(001) in two orientations, (001) or (111); the preferred orientation is critically dependent on the growth conditions. In the former orientation, the lattice mismatch between substrate and epilayer is −14.6%, whereas in the latter, the CdTe grows so that $[1\bar{1}0]$CdTe is parallel to $[1\bar{1}0]$GaAs (−14.6% misfit) but $[11\bar{2}]$CdTe is parallel to [110]GaAs (+0.7% misfit). The results described here have been taken from both (111)- and (001)-oriented CdTe systems grown by molecular beam epitaxy. Previous analysis (*13*, *14*) carried out with high-resolution electron microscopy (HREM) has provided important and detailed information on, for example, the relative density of different defect structures and the angle of substrate tilt. However, it has not proved possible to provide direct structural information with Z sensitivity on the precise sublattice arrangements at interfaces and defects.

The method of Z-contrast imaging (*15*) in STEM is an incoherent imaging technique in which, when the crystalline specimens are oriented along principal zone axes, the recorded image can be interpreted simply as a convolution between an object function (the Z-sensitive columnar scattering cross section into the high-angle electron detector) and a point spread function (the incident electron probe intensity). In this way, the recent development of a 300-kV STEM with a 1.3 Å probe has facilitated the direct observation of structural polarity in the sublattice in all compound semiconductor materials (including GaAs) oriented along ⟨110⟩ (*16*). In contrast to HREM, in which image contrast can change as a function of beam defocus and specimen thickness, Z-contrast imaging provides immediately intuitive data at atomic resolution (that is, regions of high intensity can be directly correlated to atomic column positions) (Fig. 1A). Furthermore, as a result of image incoherence it is possible, by applying the technique of maximum entropy (*17*, *18*), to retrieve the "most likely" Z-contrast object function from each image. A detailed discussion of the implementation and subsequent interpretation of the maximum entropy approach as applied to the study of Z-contrast images is given in (*19*). This method is robust and insensitive to small specimen tilts and exact probe defocus, and the retrieved object function contains quantitative positional and compositional information. It comprises an array of narrow intensity spikes (effectively delta functions) located at the atomic column sites, each with a strength related to that column's scattering power (Fig. 1B). This information is more readily presented by convolution with a small Gaussian probe to form a "maximum entropy image" (Fig. 1C). In this way, quantitative object function information is preserved, and it is still possible to observe structures intuitively as in Fig. 1A but in the absence of shot noise. It is by this route that an atomic resolution image of a region of CdTe in the CdTe(111)/GaAs(001) system is presented in Fig. 1D. In this material, HREM observation along [110] has indicated the presence of multiple twins parallel to the heteroepitaxial interface. In

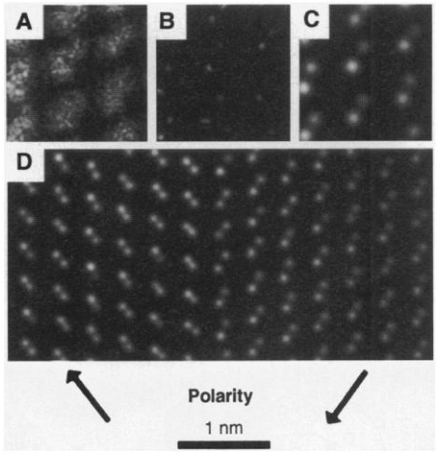

Fig. 1. (**A**) As-acquired *Z*-contrast image of CdTe in CdTe(111)/GaAs(001) viewed along the [110] projection, directly revealing sublattice polarity. (**B**) The "most likely" *Z*-contrast object function of (A) obtained by maximum entropy analysis. (**C**) Maximum entropy image of (A). (**D**) Maximum entropy image of a wider area in the same material showing a twinned region of crystal. The direction of structural polarity (marked) is continuous across the boundary. The scale marker refers to (D); (A) through (C) are enlargements showing the resolution of the dumbbells, separation 1.62 Å.

A. J. McGibbon and S. J. Pennycook, Solid State Division, Oak Ridge National Laboratory, Oak Ridge, TN 37831–6030, USA.
J. E. Angelo, Sandia National Laboratories, Livermore, CA 94550, USA.

*Present address: Department of Physics and Astronomy, University of Glasgow, Glasgow G12 8QQ, Scotland, UK.
†Present address: Materials Engineering Department, 1289 MSEE Building, Purdue University, West Lafayette, IN 47907, USA.

the same way, such features can also be observed with Z-contrast imaging but at a level of resolution at which individual atomic columns can be directly located. Clearly identifiable in the image is the structural polarity in each layer (Te brighter than Cd), which is continuous across the twin boundary. With III-V and II-VI semiconductors in which the intrinsic Z contrast between anion and cation columns is low, there is, as a result of image noise, a finite probability that a small number of dumbbells will exhibit an anomalous polarity "inversion." Thus, to discern local polarity, it generally requires information from more than an individual dumbbell. The effect of a small misorientation in the crystal with respect to the incident beam direction is a reduction of spatial resolution and Z contrast. Thus, although significant tilt can make it impossible to assign sublattice polarity, it cannot lead to an overall polarity inversion. Silicon, for example, has never shown any apparent lattice polarity.

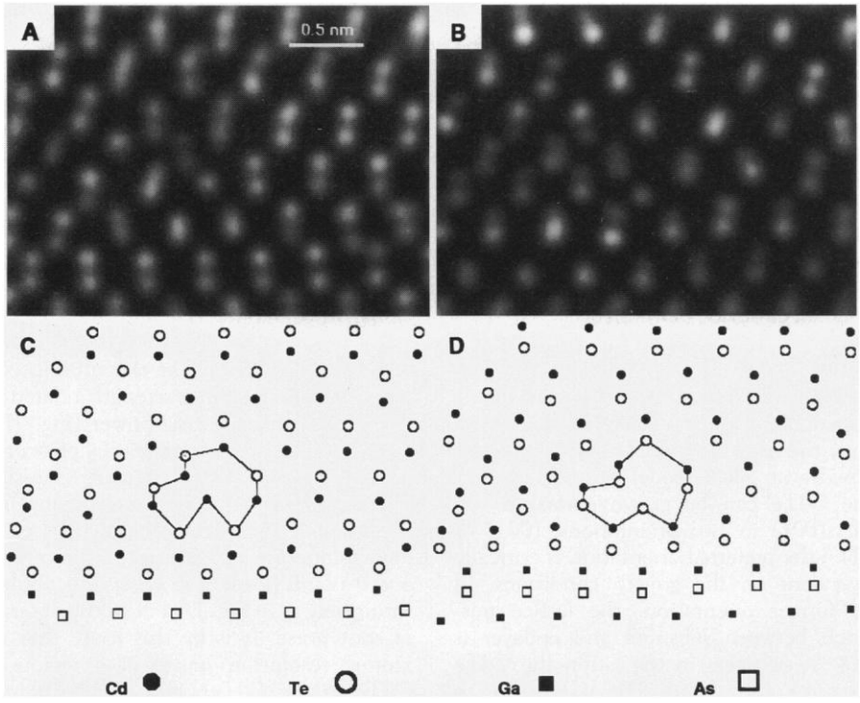

Fig. 2. Sixty-degree dislocations at the interface in CdTe(001)/GaAs(001) viewed in the (**A**) [1$\bar{1}$0] and (**B**) [110] orientations. (**C** and **D**) Schematic representations of (A) and (B), respectively. Both dislocations are of the glide set.

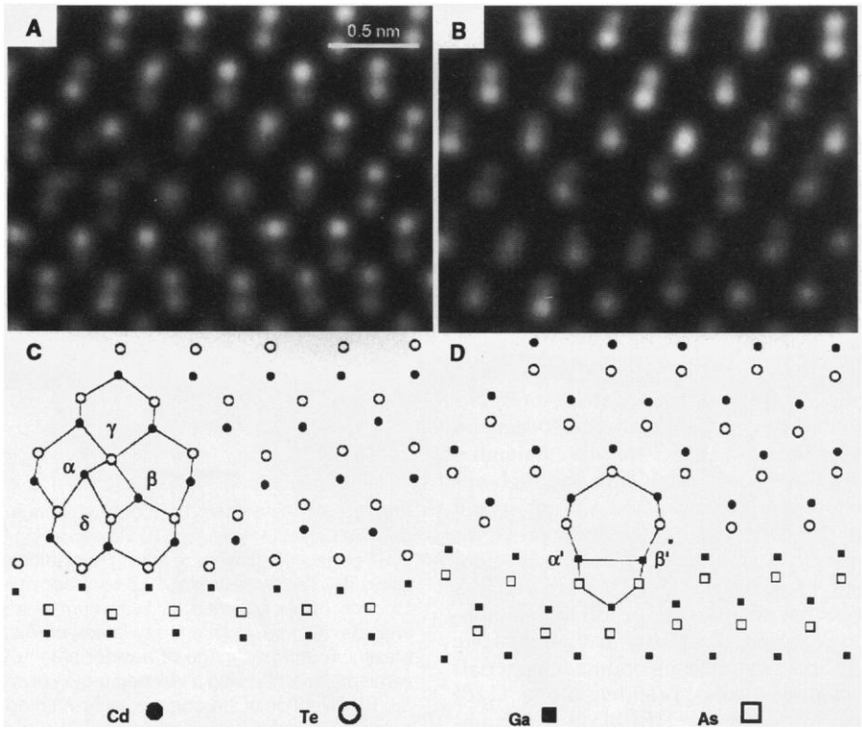

Fig. 3. Lomer dislocations at the interface in CdTe(001)/GaAs(001) viewed in the (**A**) [1$\bar{1}$0] and (**B**) [110] orientations. (**C** and **D**) Schematic representations of (A) and (B), respectively. The dislocation in (A) possesses an unexpected core structure and that in (B) is Hornstra-like.

In the analysis of the CdTe(001)/GaAs(001) system, we used Z-contrast imaging to probe microstructures at both 60° and Lomer dislocations at the interface (Figs. 2 and 3). At the dislocations cores in each of the images, the presence of local strain results in a reduction of channeling contrast and hence Z sensitivity. Column positions are, nevertheless, clear. Our strategy for determining core structures at dislocations from the Z-contrast object function is as follows: First, the interface between GaAs and CdTe is distinguished by the increase in signal intensity over one monolayer. Second, the direction of structural polarity on both sides of the interface is deduced from regions outside the core, where, as in the analysis of Fig. 1, it is directly observable. Finally, at the dislocation core, we assign column compositions consistent with the sublattice polarity in the surrounding matrix.

The dislocations shown in Fig. 2, A and B, with schematic representations in C and D, respectively, are core structures in CdTe viewed along [1$\bar{1}$0] and [110]. As expected from the growth conditions used in the fabrication of these materials (*13*), the first monolayer above the interface is occupied by Te. It can be seen that, because the two dislocations are viewed in orthogonal directions, Te occupies the upper column of each dumbbell in Fig. 2A but the lower column in Fig. 2B. According to the information in these images, the atomic arrangements correspond to perfect 60° dislocations, the core of which is located in the CdTe epilayer and not at the interface, as may have been expected. Because of the double-layer atomic arrangement of the diamond cubic lattice, two sets of 60° dislocations (glide or shuffle) with identical Burgers vectors can exist (*20*), the former showing a single atomic column at the core, the latter a dumbbell when viewed along (110). Furthermore, in compound semiconductors, the

electronic characteristics of a dislocation will vary depending on which atomic species is present at the dislocation core (*21*). From the image data alone, it is clear that both dislocations shown here are of the glide set (as were all 60° dislocations analyzed), indicating the presence of Cd-terminated dislocations along [1$\bar{1}$0] and Te-terminated dislocations along [110].

In a manner similar to that of Fig. 2, Lomer dislocations viewed along [1$\bar{1}$0] and [110] are shown in Fig. 3, A and B, respectively, with their corresponding core structures in C and D. As in the case of 60° dislocations, two possible configurations can exist that possess identical Burgers vectors. In this case, the core structure viewed along [1$\bar{1}$0] is situated above the interface and is asymmetric in nature, best described as consisting of five irregular sixfold rings surrounding a fourfold ring. The experimental evidence shows that the observed structure is unlike that of the Hornstra model (*1*), which can be described as a sevenfold ring coupled to a fivefold ring. However, atomic arrangements similar to the Hornstra model were observed along [110] but with the dislocation located exactly at the interface, implying that the two columns common to both the five- and seven-membered rings (marked α' and β') were occupied by Ga atoms. The most likely rationalization of the observed atomic arrangements in the asymmetric structure is that Cd columns α and β each possess one dangling bond per atom and that there is also a small shear (positive for α and negative for β or vice versa) of each column along [1$\bar{1}$0] (parallel to the dislocation line direction) to accommodate a skewed tetrahedral bonding configuration for atoms in Te columns γ and δ. These data suggest that, possibly as a result of the highly polar nature of the CdTe, the Hornstra structure is not energetically favored when a dislocation occurs entirely within the material.

The nature of the observed structures in both the 60° and Lomer dislocations gives rise to a number of questions relating to, for example, dislocation energy, the chemical bonding in each region, the electrical activity, and the possible existence of a small number of stabilizing impurity atoms at dislocation cores. Such phenomena can now also be investigated experimentally with atomic resolution parallel-detection electron energy-loss spectroscopy (*22*). It should be stressed that although asymmetric Lomer dislocation core structures in both Si (*5*) and compound semiconductor (*2*) systems have been proposed, they differ from that observed here because it has not hitherto been possible to obtain direct evidence of column arrangements solely from experimental data. A key advantage of the Z-contrast technique is that further theoretical and experimental investigations into the physics and chemistry of such atomic configurations can use the directly observed structures as a firm foundation from which to proceed. Our observation that core structures in polar materials can be significantly different from those in nonpolar materials should enhance the understanding of compound semiconductor heterostructures. The ability to determine dislocation core structures directly is expected to have a major impact in many other fields of materials science, leading perhaps to the understanding and control of brittleness, the key factor limiting the performance of structural materials.

REFERENCES AND NOTES

1. J. Hornstra, *J. Phys. Chem. Solids* **5**, 129 (1958).
2. F. Louchet and J. Thibault-Desseaux, *Rev. Phys. Appl.* **22**, 207 (1987).
3. K. Masuda, K. Kojima, T. Hoshino, *Jpn. J. Appl. Phys.* **22**, 1240 (1983).
4. A. S. Nandedkar and J. Narayan, *Philos. Mag. A* **61**, 873 (1990).
5. A. Bourret, J. Desseaux, A. Renault, *ibid.* **45**, 1 (1982).
6. S. H. Shin *et al.*, *J. Vac. Sci. Technol. B* **10**, 1492 (1992).
7. R. Balcerak and L. Brown, *ibid.*, p. 1353.
8. N. Otsuka *et al.*, *Appl. Phys. Lett.* **48**, 248 (1986).
9. S. Tatarenko *et al.*, *Appl. Surf. Sci.* **41–42**, 470 (1989).
10. G. Biasiol *et al.*, *Phys. Rev. Lett.* **69**, 1283 (1992).
11. M. Marsi *et al.*, *J. Appl. Phys.* **71**, 2048 (1992).
12. T. T. Cheng *et al.*, *J. Cryst. Growth* **135**, 409 (1994).
13. J. E. Angelo, W. W. Gerberich, G. Bratina, L. Sorba, A. Franciosi, *ibid.* **130**, 459 (1993).
14. J. E. Angelo *et al.*, *Philos. Mag. Lett.* **67**, 279 (1993).
15. S. J. Pennycook and D. E. Jesson, *Acta Metall. Mater.* **40**, S149 (1992).
16. A. J. McGibbon, S. J. Pennycook, Z. Wasilewski, *Mater. Res. Soc. Symp. Proc.* **326**, 299 (1994).
17. The maximum-entropy method of Gull and Skilling (*18*) calculates the most likely object function (that with maximum entropy), which, when convoluted with a point spread function, best matches the experimental data. The point spread function is the only additional information required by the program.
18. S. F. Gull and J. Skilling, *IEE Proc. F* **131**, 646 (1984).
19. A. J. McGibbon, S. J. Pennycook, D. E. Jesson, in preparation.
20. J. P. Hirth and J. Lothe, *Theory of Dislocations* (Wiley, New York, ed. 2, 1982), pp. 373–383.
21. P. Haasen, *Acta Metall.* **5**, 598 (1957).
22. M. M. McGibbon *et al.*, *Science* **266**, 102 (1994).

23. We would like to thank T. C. Estes and J. T. Luck for technical assistance. This research was sponsored by the Division of Materials Sciences, U.S. Department of Energy, under contracts DE-AC05-840R21400 and DC-AC04-94AL85000 with Martin Marietta Energy Systems and was supported in part by an appointment to the Oak Ridge National Laboratory Postdoctoral Research Program administered by the Oak Ridge Institute for Science and Education.

8 February 1995; accepted 31 May 1995

Sterkfontein Member 2 Foot Bones of the Oldest South African Hominid

Ronald J. Clarke and Phillip V. Tobias*

Four articulating hominid foot bones have been recovered from Sterkfontein Member 2, near Johannesburg, South Africa. They have human features in the hindfoot and strikingly apelike traits in the forefoot. While the foot is manifestly adapted for bipedalism, its most remarkable characteristic is that the great toe (hallux) is appreciably medially diverged (varus) and strongly mobile, as in apes. Possibly as old as 3.5 million years, the foot provides the first evidence that bipedal hominids were in southern Africa more than 3.0 million years ago. The bones probably belonged to an early member of *Australopithecus africanus* or another early hominid species.

Bipedalism was attained early in hominid evolution. Skeletal adaptations for this form of stance and gait are apparent in the pelvic girdle, hip complex, knee joint, and foot of African apemen, the australopithecines (*1*). The locomotor apparatus of early hominids was derived from that of quadrupedal, arboreal ancestors (*2*). There is debate whether arboreal adaptations persisted in australopithecines and, if so, whether arboreal activities were part of their locomotor repertoire or whether such traits were simply evolutionary baggage (*3*, *4*).

A discovery at Sterkfontein near Johannesburg, South Africa, of four foot bones provides evidence that the australopithecine foot possessed an apelike great toe that diverged from the other toes and was highly mobile. The foot bones (Stw 573) were found among mammalian remains that had been extracted from Dump 20 in 1980. Although they were not found in situ, there is no doubt that they came from Member 2 of the six-member Sterkfontein Formation (*5*, *6*). The approximately 670 hominid specimens recovered from Sterkfontein to date have come exclusively from Members 4 and 5 (*7*).

Palaeo-Anthropology Research Unit, Department of Anatomy and Human Biology, University of the Witwatersrand Medical School, 7 York Road, Parktown, Johannesburg 2193, South Africa.

*To whom correspondence should be addressed.